sustainability

MDPI

Article

Collaborative Optimization Scheduling of Source-Network-Load-Storage System Based on Ladder-Type Green Certificate–Carbon Joint Trading Mechanism and Integrated Demand Response

Zhenglong Wang [1], Jiahui Wu [1,*], Yang Kou [2], Menglin Zhang [1] and Huan Jiang [2]

[1] State Centre for Engineering Research, Ministry of Education for Renewable Energy Generation and Grid-Connected Control, Xinjiang University, Urumqi 830047, China; wangzhenglong0123@163.com (Z.W.); 17881155952@163.com (M.Z.)
[2] Electric Power Research Institute of State Grid Xinjiang Electric Power Co., Ltd., Urumqi 830011, China; kouy0081@163.com (Y.K.); 17590035151@163.com (H.J.)
* Correspondence: wjh229@xju.edu.cn

Abstract: To fully leverage the potential flexibility resources of a source-network-load-storage (SNLS) system and achieve the green transformation of multi-source systems, this paper proposes an economic and low-carbon operation strategy for an SNLS system, considering the joint operation of ladder-type green certificate trading (GCT)–carbon emission trading (CET), and integrated demand response (IDR). Firstly, focusing on the load side of electricity–heat–cooling–gas multi-source coupling, this paper comprehensively considers three types of flexible loads: transferable, replaceable, and reducible. An IDR model is established to tap into the load-side scheduling potential. Secondly, improvements are made to the market mechanisms: as a result of the division into tiered intervals and introduction of reward–penalty coefficients, the traditional GCT mechanism was improved to a more constraining and flexible ladder-type GCT mechanism. Moreover, the carbon offset mechanism behind green certificates serves as a bridge, leading to a GCT-CET joint operation mechanism. Finally, an economic low-carbon operation model is formulated with the objective of minimizing the comprehensive cost consisting of GCT cost, CET cost, energy procurement cost, IDR cost, and system operation cost. Simulation results indicate that by effectively integrating market mechanisms and IDR, the system can enhance its capacity for renewable energy penetration, reduce carbon emissions, and achieve green and sustainable development.

Keywords: green certificate trading; carbon trading; integrated demand response; source-network-load-storage system; low-carbon economy

Citation: Wang, Z.; Wu, J.; Kou, Y.; Zhang, M.; Jiang, H. Collaborative Optimization Scheduling of Source-Network-Load-Storage System Based on Ladder-Type Green Certificate–Carbon Joint Trading Mechanism and Integrated Demand Response. *Sustainability* **2024**, *16*, 10104. https://doi.org/10.3390/su162210104

Academic Editor: Seung-Hoon Yoo

Received: 12 October 2024
Revised: 8 November 2024
Accepted: 18 November 2024
Published: 19 November 2024

1. Introduction

Addressing climate change and achieving energy transition have become international consensus [1]. Against the backdrop of the "dual carbon" goals, China urgently needs to construct a more efficient system for integrating new energy sources and scientifically controlling carbon emissions [2]. SNLS can enable efficient energy utilization and has gradually become a key means of promoting energy transition [3]. Simultaneously, with the development of market mechanisms and the increase in flexible resources on the load side, determining how to fully utilize their scheduling capabilities to support the green transition of an SNLS system has become a pressing issue [4,5]. Therefore, this paper aims to provide theoretical support for achieving the economic and low-carbon optimization of an SNLS system by utilizing both market mechanisms and IDR.

At present, the methods for achieving economic and low-carbon operation of systems mainly fall into two categories [6]: technological and market-based approaches. On

the technological front, research has focused on carbon capture technologies, power-to-gas (P2G) technologies, and waste heat utilization technologies, among others [7–9]. On the market side, initiatives such as the renewable portfolio standard (RPS), green certificate trading (GCT), and carbon emission trading (CET) mechanisms have been explored. Yang et al. [10] proposed a scheduling strategy for an electric–thermal integrated system taking into account carbon capture technology, which can effectively reduce wind power curtailment and carbon emissions. Chen et al. [11] proposed an optimization model that combines combined heat and power (CHP), carbon capture, and P2G, enhancing the coupling between different energy sources; Liu and Li [12] utilized the Kalina cycle to recover waste heat from the energy production process, effectively improving energy utilization efficiency; Chen et al. [13] fully absorbed the excess heat from the operation of gas turbines by installing waste heat boilers (WHBs). These technological approaches can to some extent control the economics and carbon emission of energy systems, but the increased complexity of the units also raises operational costs and maintenance difficulty.

The combination of the RPS and GCT can effectively enhance a system's capacity for absorbing renewable energy [14]. Additionally, implementing the CET mechanism can curb carbon emission levels, further leveraging the market's scheduling capabilities; Li et al. [15] consider the CET cost in the objective function, leading the system to preferentially select equipment with lower carbon emission levels, thus enhancing environmental benefits; Zhu et al. [16] effectively constrained carbon emission levels by introducing the ladder-type CET mechanism; Gao et al. [17] verified that the ladder-type CET mechanism, which considers CET cost, can most effectively control both the economic and environmental levels; Zhang et al. [18] comprehensively consider both CET and GCT market mechanisms, ensuring the economical and low-carbon operation of a virtual power plant. Integrating both market mechanisms can balance a system's economy and low-carbon goals. However, traditional market mechanisms still lack sufficient constraints and flexibility, and barriers between different market mechanisms need to be addressed.

The load aspect of an SNLS system possesses abundant flexible resources available for scheduling. Traditional demand response mechanisms guide load participation through pricing and incentive measures to achieve supply–demand matching [19]. Chen et al. [20] successfully reduced electricity cost and nighttime peak loads by scheduling flexible resources in residential buildings; Bin et al. [21] established an optimization scheduling model considering price-based DR, which reduced the microgrid's electricity cost during peak hours; Guo and Xu [22] comprehensively consider both CET and DR mechanisms, effectively reducing carbon emissions and operating cost. The rational use of the DR mechanism can enhance a system's scheduling capabilities. However, determining how to effectively utilize the complementary relationships between different energy sources to achieve integrated demand response still requires further discussion and validation.

In summary, while traditional scheduling models have provided foundational work in enhancing an SNLS system's performance, there remain limitations in flexibility and economic efficiency within current market and demand response mechanisms. This paper addresses these limitations by proposing an innovative scheduling strategy for SNLS that integrates a ladder-type GCT-CET joint operation mechanism and IDR. Through this novel framework, we aim to provide an adaptable and economically viable solution that enhances renewable energy utilization and emission reductions within SNLS systems. This study establishes a more flexible ladder-type GCT mechanism to incentivize renewable energy consumption and develops a joint operational framework for GCT and CET to eliminate barriers between different market mechanisms. Additionally, by implementing the IDR mechanism, this study leverages the response capacity on the load side to further optimize the supply–demand balance in the SNLS system. The proposed strategy's effectiveness is substantiated through comparative case studies and sensitivity analyses, affirming its role in advancing sustainable scheduling practices. The primary innovations and contributions of this study can be outlined as follows:

(1) By dividing the number of green certificates into multiple sub-intervals and introducing reward–penalty coefficients, a ladder-type GCT mechanism is proposed, strengthening the willingness of the SNLS system to absorb renewable energy.
(2) A joint operation mechanism between GCT and CET was constructed through the carbon offset mechanism behind green certificates, effectively controlling the system's operating costs and enhancing environmental benefits.
(3) Fully exploiting the coupling relationships among various loads such as electricity, heat, gas, and cooling, and considering the characteristics of transferable, replaceable, and reducible flexible loads, an IDR model was established to alleviate the supply–demand balance in the SNLS systems.
(4) With the objective function of minimizing the comprehensive cost of the SNLS system, the proposed scheduling strategy's effectiveness in economic low-carbon optimization was verified through six case comparisons and sensitivity analyses.

2. SNLS System Considering Ladder-Type GCT-CET Joint Operation and IDR Mechanisms

2.1. Architecture of the SNLS System

The SNLS system designed in this paper effectively accounts for the regulation capabilities of the energy side, demand side, and storage side. Figure 1 illustrates the operational framework of the SNLS system.

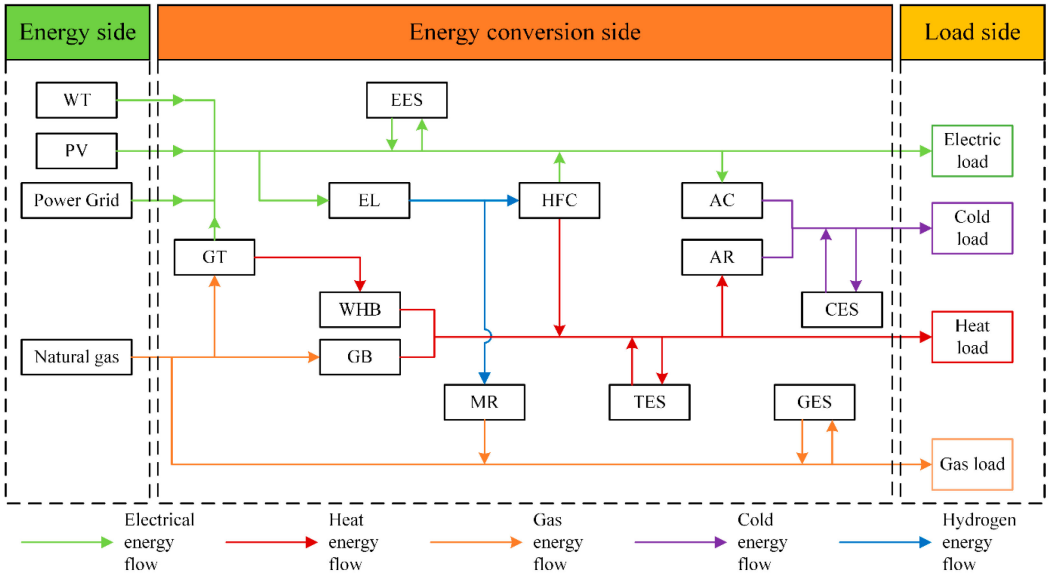

Figure 1. Schematic diagram of SNLS system operation.

According to Figure 1, the energy side of the SNLS system takes into account wind turbine (WT), photovoltaic (PV), upper-level power grids, and upper-level gas networks. The energy conversion side comprises hydrogen multi-utilization equipment consisting of an electrolyzer (EL), a methane reactor (MR), and a hydrogen fuel cell (HFC); CHP equipment composed of a gas turbine (GT) and waste heat boiler (WHB); and a gas boiler (GB), an air conditioner (AC), and an absorption refrigerator (AR). Energy storage units include multiple types of storage devices such as electrical energy storage (EES), cold energy storage (CES), thermal energy storage (TES), and gas energy storage (GES).

2.2. GCT Mechanism

2.2.1. The Principle of GCT Mechanism

The renewable portfolio standard (RPS) is a government-established policy aimed at reducing the dependence on conventional energy and promoting the utilization of renewable energy. Relevant authorities set clear targets and standards for environmental

objectives under the RPS, where the energy suppliers or power companies are required to use a specific percentage of renewable energy, such as wind, solar, hydro, etc., in their overall energy production. These assessing entities must demonstrate that they have met or exceeded the government-mandated quotas for renewable energy, giving rise to the GCT mechanism.

Under the GCT mechanism, renewable energy producers or consumers can obtain green certificates, proving that the energy they produce or utilize is based on renewable energy resources. When the actual quantity of green certificates exceeds the quota, certificate holders can sell the surplus to gain economic benefits. Conversely, if the quantity of green certificates held is insufficient, holders must purchase certificates to fulfill the quota requirements. The joint operation of RPS and GCT can not only incentivize energy suppliers and power generation companies to invest in renewable energy projects but also increase users' willingness to consume renewable energy and contribute to social economic growth and green transformation.

The operating principle of GCT is illustrated in Figure 2.

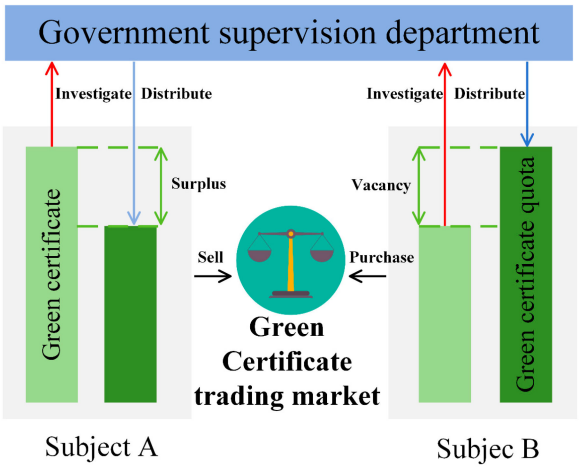

Figure 2. Operational principle of GCT mechanism.

2.2.2. A Ladder-Type GCT Mechanism with Stronger Binding Force and Flexibility

The proposed ladder-type GCT mechanism is designed to enhance both the binding force and flexibility of trading green certificates compared to the conventional GCT models. The selection of reward–penalty coefficients is based on empirical market behavior and regulatory requirements, ensuring that the participants are effectively incentivized while maintaining manageable overall costs. These coefficients encourage renewable energy utilization, while ensuring that the participants can handle the costs associated with exceeding or failing to meet the quota.

This mechanism divides GCT costs into three distinct stages: (i) reward, (ii) conventional, and (iii) penalty. In the reward stage, participants can sell surplus green certificates for additional revenue when they hold more than the set quota, thereby promoting the utilization of renewable energy sources and boosting profits. In the conventional stage, costs are calculated using the traditional GCT mechanism, offering a familiar approach for participants. Conversely, when the number of certificates falls below the required quota, the penalty stage is triggered, imposing higher trading prices and increasing the associated costs. This tiered structure ensures that non-compliance incurs progressively severe financial consequences, thereby enforcing stronger constraints on renewable energy consumption. The rationale behind this tiered structure lies in its ability to provide more nuanced incentives compared to the conventional linear models. By establishing distinct phases—reward, conventional, and penalty—the mechanism allows for customized responses to market changes, fostering an adaptable system that is better suited for integrat-

ing renewable energy resources. This flexible approach aligns with government policies aimed at enhancing renewable energy adoption and consumption.

The ladder-type GCT model is as follows:

$$\begin{cases} Q_n = \alpha_P \cdot \alpha_z \cdot \sum_{t=1}^{T} P_{\mathrm{e},L}(\mathrm{t}) \\ Q_h = \alpha_z \cdot \sum_{t=1}^{T} \left[P_{wind}(\mathrm{t}) + P_{\mathrm{pv}}(\mathrm{t})\right] \end{cases} \tag{1}$$

where Q_n represents the green certificate quota; α_P denotes the quota coefficient of green certificates; $P_{\mathrm{e},L}(\mathrm{t})$ is the total electrical load; Q_h represents the quantity of green certificates obtained; α_z represents the green certificate conversion coefficient; $P_{wind}(\mathrm{t})$ is the electrical power produced by the WT; $P_{\mathrm{pv}}(\mathrm{t})$ denotes the electrical power produced by the PV.

$$Q_{\mathrm{GCT}} = Q_n - Q_h \tag{2}$$

$$\lambda_{\mathrm{GCT}} = \begin{cases} -\mathrm{C}_{\mathrm{GCT}} \cdot (2+3\mathrm{e}) \cdot \mathrm{d} + \mathrm{C}_{\mathrm{GCT}} \cdot (1+3\mathrm{e}) \cdot (Q_{\mathrm{GCT}} + 2\mathrm{d}),\ Q_{\mathrm{GCT}} \le -2\mathrm{d} \\ -\mathrm{C}_{\mathrm{GCT}} \cdot (1+\mathrm{e}) \cdot \mathrm{d} + \mathrm{C}_{\mathrm{GCT}} \cdot (1+2\mathrm{e}) \cdot (Q_{\mathrm{GCT}} + \mathrm{d}), -2\mathrm{d} < Q_{\mathrm{GCT}} \le -\mathrm{d} \\ \mathrm{C}_{\mathrm{GCT}} \cdot (1+\mathrm{e}) \cdot (Q_{\mathrm{GCT}}), -\mathrm{d} < Q_{\mathrm{GCT}} \le 0 \\ \mathrm{C}_{\mathrm{GCT}} \cdot (Q_{\mathrm{GCT}}), 0 < Q_{\mathrm{GCT}} \le \mathrm{d} \\ \mathrm{C}_{\mathrm{GCT}} \cdot \mathrm{d} + \mathrm{C}_{\mathrm{GCT}} \cdot (1+\mathrm{u}) \cdot (Q_{\mathrm{GCT}} - \mathrm{d}),\ \mathrm{d} < Q_{\mathrm{GCT}} \le 2\mathrm{d} \\ \mathrm{C}_{\mathrm{GCT}} \cdot (2+\mathrm{u}) \cdot \mathrm{d} + \mathrm{C}_{\mathrm{GCT}} \cdot (1+2\mathrm{u}) \cdot (Q_{\mathrm{GCT}} - 2\mathrm{d}),\ Q_{\mathrm{GCT}} > 2\mathrm{d} \end{cases} \tag{3}$$

where Q_{GCT} represents the quantity of green certificates either sold or purchased; λ_{GCT} is the cost of GCT; $\mathrm{C}_{\mathrm{GCT}}$ is the basic price of green certificates; e represents the reward coefficient of ladder-type GCT; u represents the price increase range of ladder-type GCT; d is the interval length.

2.3. CET Mechanism

2.3.1. The Principle of CET Mechanism

The CET mechanism is a market-based strategy designed to reduce carbon emissions. Under this framework, the government establishes a limit on carbon emissions and allocates Carbon Emission Allowances (CEAs) to participants such as factories, power plants, and other sources of emissions. Each participant receives a specific CEA, which represents the maximum amount of emissions allowed. If a participant's actual emissions exceed their allocated CEA, they are required to purchase additional CEA from the market to cover the excess emissions. This generates demand, leading to price fluctuations driven by market dynamics such as supply, demand, and regulatory policies. Conversely, participants who emit less than their allocated CEA can sell their surplus CEA for profit, thereby incentivizing emission reductions and fostering the advancement of low-carbon technology.

Economic trends, policy changes, and the integration of renewable energy will influence carbon pricing under the CET mechanism. By incorporating these real-world factors, developing robust models that accurately simulate market conditions and participant behavior can help drive carbon reduction and promote strategic investment in clean energy technologies.

The operating principle of the CET mechanism is illustrated in Figure 3.

2.3.2. The CEA Model Based on Baseline Method

In the SNLS system established in this paper, carbon emission sources include purchased electricity, CHP units, GB units, and gas loads. This study adopts a baseline approach, allocating CEAs for free based on historical emission data and performance benchmarks, ensuring that each participant receives CEAs that reflect their operational capacity and past emissions. The allocation process considers various factors, such as the following:

(1) Quota coefficient: Quantifying the quota for each entity using appropriate coefficients ensures an accurate assessment of the environmental impact of different energy production and consumption methods.

(2) Regulatory Adjustments: The CEA allocation method aligns with government regulations and targets, creating a flexible framework capable of adapting to policy changes aimed at lowering carbon emissions.

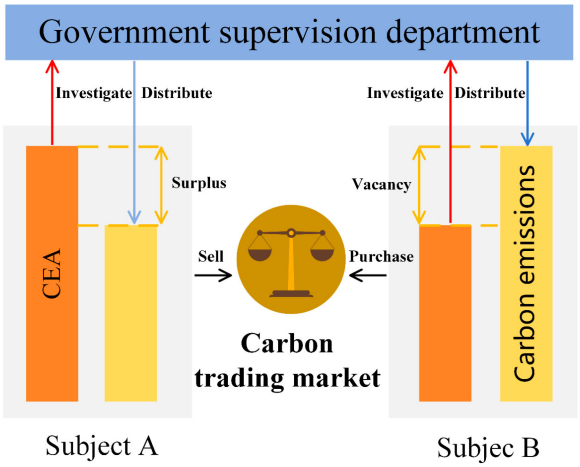

Figure 3. Operational principle of CET mechanism.

The specific model for calculating the CEA allocation is as follows:

$$\begin{cases} E^{p}_{\text{total}} = E^{p}_{Grid} + E^{p}_{CHP} + E^{p}_{GB} + E^{p}_{g,L} \\ E^{p}_{Grid} = \sigma_e \cdot \sum_{t=1}^{T} P_{Grid}(\text{t}) \\ E^{p}_{CHP} = \sigma_h \cdot \sum_{t=1}^{T} \left[\tau_{\text{CHP}} P^{\text{e}}_{\text{CHP}}(t) + P^{\text{h}}_{\text{CHP}}(t)\right] \\ E^{p}_{GB} = \sigma_h \cdot P^{\text{h}}_{\text{GB}}(t) \\ E^{p}_{g,L} = \sigma_{g,L} \cdot P_{g,L}(\text{t}) \end{cases} \tag{4}$$

where E^{p}_{total} represents the total CEA of the SNLS system; E^{p}_{Grid} is the CEA for purchased electricity; E^{p}_{CHP}, E^{p}_{GB}, and $E^{p}_{g,L}$ represent the CEAs for CHP units, GB units, and consuming gas loads, respectively; σ_e, σ_h, and $\sigma_{g,L}$ are the CEA quota coefficients of electricity generation, heat generation, and gas consumption load, respectively; τ_{CHP} is the electro-thermal conversion coefficient of the CHP units.

2.3.3. Actual Carbon Emission Model Considering Gas Load and MR

Currently, most studies do not accurately account for the carbon emissions generated from the gas loads. This paper fills this research gap by improving the carbon emission assessment model. Additionally, the impact of the Sabatier reaction in the MR unit, which converts carbon dioxide into methane, is also considered. This reaction indirectly reduces carbon emissions and holds significant value in carbon cycling and hydrogen economy. In this study, the improved carbon emission model includes specific parameters related to carbon emissions from the gas loads and the net reduction in carbon emissions from the Sabatier reaction. This approach ensures that the model reflects the complexities of the real world and enhances its applicability in assessing the environmental impact of the SNLS system.

Given that wind power and photovoltaic are clean sources of energy, their carbon emissions can be considered close to zero. Based on this, the improved carbon emission model is shown as follows:

$$\begin{cases} E_{\text{total}}^{CO2} = E_{Grid}^{CO2} + E_{CHP}^{CO2} + E_{GB}^{CO2} + E_{g,L}^{CO2} - E_{MR}^{CO2} \\ E_{Grid}^{CO2} = \theta_{\text{e}} \cdot \sum_{t=1}^{T} P_{Grid}(\text{t}) \\ E_{CHP}^{CO2} = \theta_{\text{h}} \cdot \sum_{t=1}^{T} \left[\tau_{\text{CHP}} P_{\text{CHP}}^{\text{e}}(t) + P_{\text{CHP}}^{\text{h}}(t)\right] \\ E_{GB}^{CO2} = \theta_{\text{h}} \cdot P_{\text{GB}}^{\text{h}}(t) \\ E_{g,L}^{CO2} = \theta_{g,L} \cdot P_{g,L}(\text{t}) \\ E_{MR}^{CO2} = \theta_{\text{MR}} \cdot \sum_{t=1}^{T} P_{\text{MR}}^{\text{g}}(t) \end{cases} \tag{5}$$

where E_{total}^{CO2} represents the overall carbon emission of the SNLS system; E_{Grid}^{CO2}, E_{CHP}^{CO2}, E_{GB}^{CO2}, and $E_{g,L}^{CO2}$ are the carbon emissions from electricity purchased from the superior power grid, CHP units, GB units, and consuming gas loads, respectively; θ_{e}, θ_{h}, and $\theta_{g,L}$ are the carbon emission intensity per unit of electricity production, per unit of heat production, and per unit of gas load consumption, respectively; E_{MR}^{CO2} represents the reduced carbon emissions from MR; θ_{MR} is the reduced carbon emissions when MR generates unit gas power.

2.3.4. Ladder-Type CET Mechanism

To better regulate the carbon emission levels, a ladder-type CET mechanism is employed in this study that introduces greater flexibility and transparency. This mechanism establishes the CEA as a benchmark, segmenting carbon emissions into multiple tiers to reflect the costs associated with emission levels. As the carbon emissions increase, the penalty coefficient causes the cost of purchasing additional CEA to rise gradually. This provides a strong economic incentive for participants to reduce their emissions. Conversely, when participants reduce their emissions, the reward coefficient enables them to receive greater benefits, thereby promoting proactive carbon management measures. This model acknowledges the fluctuating nature of carbon prices in the real world, providing a more robust framework for participants to navigate the complexities of carbon trading.

The ladder-type CET model is outlined as follows:

$$E_{CET} = E_{CO2} - E_P \tag{6}$$

$$\lambda_{\text{CET}} = \begin{cases} -\text{C}_{\text{CET}} \cdot (2+3\beta) \cdot \text{l} + \text{C}_{\text{CET}} \cdot (1+3\beta) \cdot (E_{CET} + 2\text{l}),\ E_{CET} \le -2\text{l} \\ -\text{C}_{\text{CET}} \cdot (1+\beta) \cdot \text{l} + \text{C}_{\text{CET}} \cdot (1+2\beta) \cdot (E_{CET} + \text{l}), -2\text{l} \le E_{CET} < -\text{l} \\ \text{C}_{\text{CET}} \cdot (1+\beta) \cdot (E_{CET}), -\text{l} \le E_{CET} < 0 \\ \text{C}_{\text{CET}} \cdot (E_{CET}),\ 0 < E_{CET} \le \text{l} \\ \text{C}_{\text{CET}} \cdot \text{l} + \text{C}_{\text{CET}} \cdot (1+\varepsilon) \cdot (E_{CET} - \text{l}),\ \text{l} < E_{CET} \le 2\text{l} \\ \text{C}_{\text{CET}} \cdot (2+\varepsilon) \cdot \text{l} + \text{C}_{\text{CET}} \cdot (1+2\varepsilon) \cdot (E_{CET} - 2\text{l}),\ E_{CET} > 2\text{l} \end{cases} \tag{7}$$

where E_{CET} is the carbon trading volume; λ_{CET} denotes the CET cost; C_{CET} is the carbon trading basic price; β denotes the reward coefficient for ladder-type CET; ε represents the price increase range of ladder-type CET; l is the interval length of ladder-type CET.

2.4. Combined GCT-CET Operation Mechanism

The green certificates record the carbon reduction benefits behind green energy. In this paper, the surplus green certificates after the completion of the green certificate quotas are divided into two parts: one part continues to engage in the green certificate market to earn GCT revenue, while the other part offsets some carbon emissions in carbon trading by considering the carbon emission reduction behind the green certificate, thereby indirectly engaging in the carbon trading market to obtain carbon emission reduction benefits. This mechanism uses green certificates as a bridge to link two different mechanisms, accu-

rately depicting the differences in carbon emission from various energy sources, thereby increasing the system's willingness to choose green energy.

The GCT-CET joint operation mechanism is depicted in Figure 4.

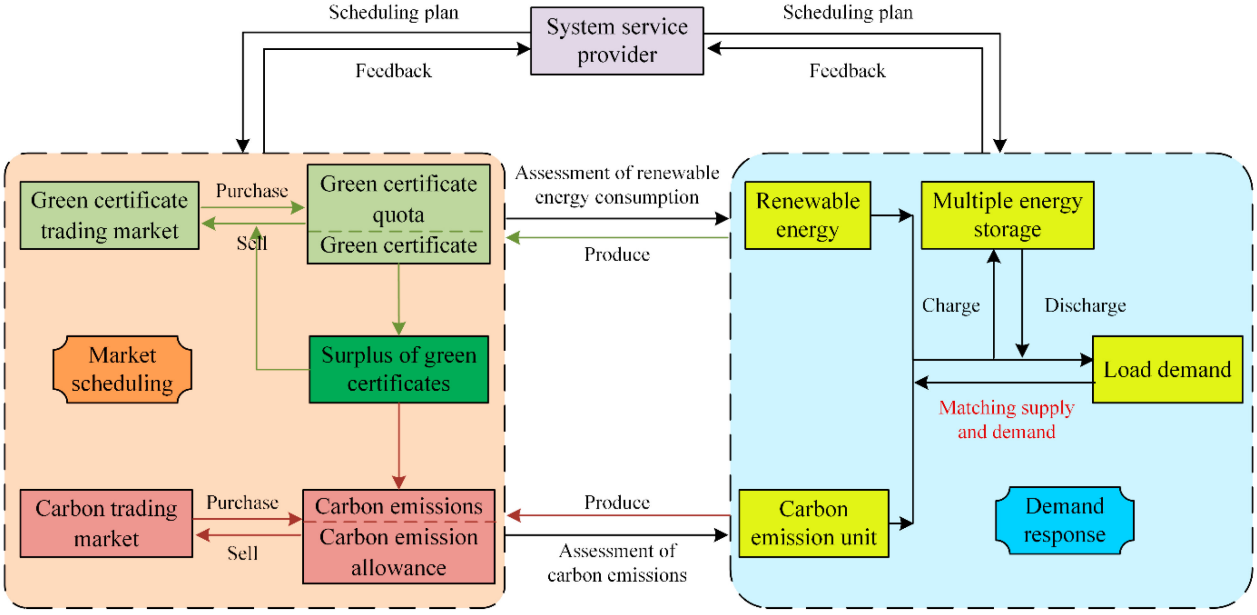

Figure 4. Joint operating principle of the GCT and CET mechanism.

The mathematical model for the GCT-CET joint operation mechanism is as follows:

$$\begin{cases} Q^* = Q_h - Q_n \\ Q^* > 0 \\ Q^* = Q_{GCT} + Q_z \end{cases} \tag{8}$$

where Q^* represents the surplus green certificate after meeting the green certificate quota; Q_{GCT} denotes the surplus green certificate participating in the green certificate trading market; Q_z is the surplus green certificate participating in the carbon offset mechanism.

Since wind power, solar power, and other clean energy sources are considered to produce virtually no carbon emissions during production and utilization, this paper sets their carbon emission intensity to zero. Therefore, the carbon emission reduction effect of green energy represented by green certificates is equivalent to offsetting the carbon emissions of an equivalent amount of coal-fired power production. When green certificates participate in the carbon offset mechanism, the corresponding quantity needs to be deducted from the surplus green certificates, and the carbon trading volume should be adjusted accordingly.

The carbon offset mechanism model is presented as follows:

$$\begin{cases} \sum\limits_{t=1}^{T} P_{GCT}(\mathrm{t}) = \dfrac{Q_z}{\alpha_z} \\ E_{Green}^{CO2} = \sum\limits_{t=1}^{T} \cdot \theta_e \cdot P_{GCT}(\mathrm{t}) \\ E_{CET}^{*} = E_{CET} - E_{Green}^{CO2} \end{cases} \tag{9}$$

where $P_{GCT}(\mathrm{t})$ is the electricity represented by the green certificates participating in the carbon offset mechanism; E_{Green}^{CO2} denotes the amount of carbon emissions offset; E_{CET}^{*} represents carbon trading volume under the GCT-CET joint operation mechanism.

2.5. IDR Mechanism That Considers Load Diversity and Flexibility

2.5.1. The Principle of the IDR Mechanism

In this article, loads are divided into (i) non-adjustable fixed loads and (ii) flexible loads. Flexible loads are further classified as (a) transferable, (b) replaceable, and (c) reducible. The flexible loads can be adjusted to varying degrees based on their regulation characteristics. To fully tap the flexibility of resources on the demand side, the article proposes providing suitable economic compensation to encourage users to proactively adjust their energy consumption when there is a supply–demand imbalance. This methodology is designed to generate an orderly response on the demand side, enabling flexible load shifting across various time periods and enabling intelligent adjustment within a single time period, thereby enhancing the efficiency of energy utilization in the proposed SNLS system.

The loads for this study are shown as follows:

$$P_{\mathrm{i},L}(\mathrm{t}) = P^{s}_{\mathrm{i},L}(\mathrm{t}) + P^{\mathrm{z}}_{\mathrm{i},L}(\mathrm{t}) + P^{\mathrm{k}}_{\mathrm{i},L}(\mathrm{t}) + P^{\mathrm{c}}_{\mathrm{i},L}(\mathrm{t}) \tag{10}$$

where i represents four different categories of loads: electrical load, heat load, cold load, and gas load; $P_{\mathrm{i},L}(\mathrm{t})$ denotes the total load of type i; $P^{s}_{\mathrm{i},L}(\mathrm{t})$ is the stationary load of type i; $P^{\mathrm{z}}_{\mathrm{i},L}(\mathrm{t})$ denotes the transferable load of type i; $P^{\mathrm{k}}_{\mathrm{i},L}(\mathrm{t})$ represents the replaceable load of type i; $P^{\mathrm{c}}_{\mathrm{i},L}(\mathrm{t})$ is the reducible load of type i.

2.5.2. Transferable Load

Transferable loads refer to loads whose operation times can be adjusted without significantly affecting their function or user convenience. Examples of transferable loads include household appliances like washing machines and dishwashers, as well as certain industrial processes that can be rescheduled to off-peak periods. The flexibility of these loads depends on user preferences, operational constraints, and the incentive structures provided. This paper utilizes economic incentives to encourage users to reduce energy consumption during peak demand periods and increase it during valley times. This approach aims to achieve load shifting on the demand side, thereby reducing the peak–valley difference in load and effectively alleviating the system's supply–demand pressure. The mathematical model is presented as follows:

$$\begin{cases} P^{z}_{\mathrm{i},L}(\mathrm{t}) = P^{z,0}_{\mathrm{i},L}(\mathrm{t}) + \Delta P^{z}_{\mathrm{i},L}(\mathrm{t}) \\ \Delta P^{z}_{\mathrm{i},L}(\mathrm{t}) = \mathrm{r}^{z}_{\mathrm{i,in}}(\mathrm{t}) \cdot \mathrm{P}^{z}_{\mathrm{i,in}}(\mathrm{t}) - \mathrm{r}^{z}_{\mathrm{i,out}}(\mathrm{t}) \cdot \mathrm{P}^{z}_{\mathrm{i,out}}(\mathrm{t}) \\ \mathrm{r}^{z}_{\mathrm{i,in}}(\mathrm{t}) + \mathrm{r}^{z}_{\mathrm{i,out}}(\mathrm{t}) = 1 \\ \sum\limits_{t=1}^{T} \Delta P^{z}_{\mathrm{i},L}(\mathrm{t}) = 0 \\ \Delta P^{z,min}_{\mathrm{i},L}(\mathrm{t}) \le \Delta P^{z}_{\mathrm{i},L}(\mathrm{t}) \le \Delta P^{z,max}_{\mathrm{i},L}(\mathrm{t}) \end{cases} \tag{11}$$

where $P^{\mathrm{z},0}_{\mathrm{i},L}(\mathrm{t})$ represents the initial value of the transferable load for type i; $\Delta P^{z}_{\mathrm{i},L}(\mathrm{t})$ denotes the amount of transferred load for type i; $\mathrm{r}^{z}_{\mathrm{i,in}}(\mathrm{t})$ and $\mathrm{r}^{z}_{\mathrm{i,out}}(\mathrm{t})$ are the state variable of transferable load for type i; $\Delta P^{z,max}_{\mathrm{i},L}(\mathrm{t})$ and $\Delta P^{z,min}_{\mathrm{i},L}(\mathrm{t})$ denote the maximum and minimum bounds of the transferable load for type i.

2.5.3. Replaceable Load

Replaceable loads refer to energy consumption processes or devices that can switch between different energy sources without affecting their primary function. This flexibility allows the system to dynamically switch between energy sources based on availability, cost, or carbon emission impacts. This paper considers potential substitution relationships between various types of energy loads. For instance, the electric water heater can substitute for the gas water heater. Thus, under the premise of meeting the basic energy needs of users, different energies can be flexibly used to satisfy load demands, achieving load substitution.

The mathematical model is shown as follows:

$$\begin{cases} P_{i,L}^{k}(t) = P_{i,L}^{k,0}(t) + \Delta P_{i,L}^{k}(t) \\ \Delta P_{i,L}^{k}(t) = r_{i,in}^{k}(t) \cdot P_{i,in}^{k}(t) - r_{i,out}^{k}(t) \cdot P_{i,out}^{k}(t) \\ r_{i,in}^{k}(t) + r_{i,out}^{k}(t) = 1 \\ \sum_{i=1}^{4} \Delta P_{i,L}^{i}(t) = 0 \\ \Delta P_{i,L}^{k,min}(t) \le \Delta P_{i,L}^{k}(t) \le \Delta P_{i,L}^{k,max}(t) \end{cases} \tag{12}$$

where $P_{i,L}^{k,0}(t)$ represents the initial value of replaceable load for type i; $\Delta P_{i,L}^{k}(t)$ denotes the amount of substituted load for type i; $r_{i,in}^{k}(t)$ and $r_{i,out}^{k}(t)$ are the state variable of replaceable load for type i; $\Delta P_{i,L}^{k,max}(t)$ and $\Delta P_{i,L}^{k,min}(t)$ denote the maximum and minimum bounds of replaceable load for type i.

2.5.4. Reducible Load

Reducible loads refer to energy-consuming devices or processes that can temporarily reduce demand without affecting overall system performance or user comfort. These loads are typically non-essential or flexible, such as air conditioning, heating systems, or non-urgent industrial processes. The degree to which these loads can be reduced depends on factors such as user preferences, technological capabilities, and the level of incentives provided. By reducing these loads during peak periods, the system can optimize resource allocation and more effectively balance supply and demand. This paper proposes a contractual agreement wherein users can voluntarily reduce a portion of their load during peak demand periods when supply is insufficient, in exchange for economic compensation, thus alleviating the supply–demand imbalance.

The mathematical model is shown as follows:

$$\begin{cases} P_{i,L}^{c}(t) = P_{i,L}^{c,0}(t) + \Delta P_{i,L}^{c}(t) \\ \Delta P_{i,L}^{c}(t) \le 0 \\ \Delta P_{i,L}^{c,min}(t) \le \left| \Delta P_{i,L}^{c}(t) \right| \le \Delta P_{i,L}^{c,max}(t) \end{cases} \tag{13}$$

where $P_{i,L}^{c,0}(t)$ represents the initial value of the reducible load for type i; $\Delta P_{i,L}^{c}(t)$ denotes the quantity of load reduced for type i; $\Delta P_{i,L}^{c,max}(t)$ and $\Delta P_{i,L}^{c,min}(t)$ are the maximum and minimum bounds of reducible load for type i.

3. Optimal Scheduling Model of SNLS System Considering Ladder-Type GCT-CET Joint Operation and IDR

3.1. Objective Function

The objective function aims to minimize the comprehensive cost of the SNLS system, encompassing GCT cost, CET cost, energy procurement cost, IDR cost, and system operation cost.

The mathematical model is as follows:

$$\min\lambda = \min\left(\lambda_{GCT} + \lambda_{CET} + \lambda_{buy} + \lambda_{IDR} + \lambda_{s}\right) \tag{14}$$

(1) Cost of energy procurement

$$\lambda_{buy} = \sum_{t=1}^{T} \left[C_{Grid}(t) \cdot P_{Grid}(t) + C_{Gas}(t) \cdot P_{Gas}(t)\right] \tag{15}$$

where $C_{Grid}(t)$ represents the electricity price; $C_{Gas}(t)$ is the gas price.

(2) Cost of IDR

$$\lambda_{\mathrm{IDR}} = \sum_{\mathrm{i}=1}^{4} \sum_{t=1}^{T} \left(C_{\mathrm{z}} \cdot \left| \Delta P_{\mathrm{i},L}^{z}(\mathrm{t}) \right| + C_{\mathrm{k}} \cdot \left| \Delta P_{\mathrm{i},L}^{\mathrm{k}}(\mathrm{t}) \right| + C_{\mathrm{c}} \cdot \left| \Delta P_{\mathrm{i},L}^{\mathrm{c}}(\mathrm{t}) \right| \right) \tag{16}$$

where C_{z}, C_{k}, and C_{c} represent the cost of transferring, replacing, and reducing the loads, respectively.

(3) Cost of system operation

$$\lambda_s = \sum_{\mathrm{n}=1}^{\mathrm{N}} \sum_{t=1}^{T} \alpha_{\mathrm{n}} \cdot P_{\mathrm{n}}(\mathrm{t}) \tag{17}$$

where n represents different types of operation and maintenance units; N represents the total number of operation and maintenance units; α_{n} represents unit operating and maintenance costs for different units; $P_{\mathrm{n}}(\mathrm{t})$ is the output of different operation and maintenance units.

3.2. Constraints

3.2.1. Energy Output Constraints

(1) WT and PV output

$$\begin{cases} 0 \le P_{wind}(\mathrm{t}) \le P_{wind}^{*}(\mathrm{t}) \\ 0 \le P_{\mathrm{pv}}(\mathrm{t}) \le P_{\mathrm{pv}}^{*}(\mathrm{t}) \end{cases} \tag{18}$$

(2) Energy purchase

$$\begin{cases} 0 \le P_{Grid}(\mathrm{t}) \le P_{Grid}^{\max}(\mathrm{t}) \\ 0 \le P_{\mathrm{Gas}}(\mathrm{t}) \le P_{\mathrm{Gas}}^{\max}(\mathrm{t}) \end{cases} \tag{19}$$

where $P_{Grid}^{\max}(\mathrm{t})$ and $P_{\mathrm{Gas}}^{\max}(\mathrm{t})$ represent the maximum purchased electricity and gas power.

(3) Electrolyzer

$$\begin{cases} P_{\mathrm{EL}}^{\mathrm{H}}(t) = \eta_{\mathrm{EL}} P_{\mathrm{EL}}^{\mathrm{e}}(t) \\ P_{\mathrm{EL}}^{\mathrm{e,min}}(t) \le P_{\mathrm{EL}}^{\mathrm{e}}(t) \le P_{\mathrm{EL}}^{\mathrm{e,max}}(t) \end{cases} \tag{20}$$

where $P_{\mathrm{EL}}^{\mathrm{e}}(\mathrm{t})$ represents the electrical power supplied to the EL; η_{EL} denotes the hydrogen production efficiency of the EL; $P_{\mathrm{EL}}^{\mathrm{H}}(\mathrm{t})$ is the hydrogen power output produced by the EL; $P_{\mathrm{EL}}^{\mathrm{e,max}}(\mathrm{t})$ and $P_{\mathrm{EL}}^{\mathrm{e,min}}(\mathrm{t})$ represent the maximum and minimum bounds of the electrical power supplied to the EL.

(4) Hydrogen fuel cell

$$\begin{cases} P_{\mathrm{HFC}}^{\mathrm{e}}(t) = \eta_{\mathrm{HFC}}^{\mathrm{e}} P_{\mathrm{HFC}}^{\mathrm{H}}(t) \\ P_{\mathrm{HFC}}^{\mathrm{h}}(t) = \eta_{\mathrm{HFC}}^{\mathrm{h}} P_{\mathrm{HFC}}^{\mathrm{H}}(t) \\ P_{\mathrm{HFC}}^{\mathrm{H,min}} \le P_{\mathrm{HFC}}^{\mathrm{H}}(t) \le P_{\mathrm{HFC}}^{\mathrm{H,max}} \end{cases} \tag{21}$$

where $P_{\mathrm{HFC}}^{\mathrm{H}}(t)$ represents the hydrogen supplied to the HFC; $\eta_{\mathrm{HFC}}^{\mathrm{e}}$ and $\eta_{\mathrm{HFC}}^{\mathrm{h}}$ are the electrical and thermal efficiency of the HFC; $P_{\mathrm{HFC}}^{\mathrm{e}}(t)$ and $P_{\mathrm{HFC}}^{\mathrm{h}}(t)$ signify the electrical and thermal energy produced by the HFC; $P_{\mathrm{HFC}}^{\mathrm{H,max}}$ and $P_{\mathrm{HFC}}^{\mathrm{H,min}}$ represent the maximum and minimum bounds of the hydrogen supplied to the HFC.

(5) Methane reactor

$$\begin{cases} P_{\mathrm{MR}}^{\mathrm{g}}(t) = \eta_{\mathrm{MR}} P_{\mathrm{MR}}^{\mathrm{H}}(t) \\ P_{\mathrm{MR}}^{\mathrm{H,min}} \le P_{\mathrm{MR}}^{\mathrm{H}}(t) \le P_{\mathrm{MR}}^{\mathrm{H,max}} \end{cases} \tag{22}$$

where $P_{\mathrm{MR}}^{\mathrm{H}}(t)$ represents the hydrogen supplied to the MR; η_{MR} denotes the efficiency of gas production in the MR; $P_{\mathrm{MR}}^{\mathrm{g}}(t)$ is the gas power generated by the MR; $P_{\mathrm{MR}}^{\mathrm{H,max}}$ and $P_{\mathrm{MR}}^{\mathrm{H,min}}$ represent the maximum and minimum bounds of the hydrogen supplied to the MR.

(6) Combined heat and power

$$\begin{cases} P_{\mathrm{CHP}}^{\mathrm{e}}(t) = \eta_{\mathrm{CHP}}^{\mathrm{e}} P_{\mathrm{CHP}}^{\mathrm{g}}(t) \\ P_{\mathrm{CHP}}^{\mathrm{h}}(t) = \eta_{\mathrm{CHP}}^{\mathrm{h}} P_{\mathrm{CHP}}^{\mathrm{g}}(t) \\ P_{\mathrm{CHP}}^{\mathrm{g,min}} \le P_{\mathrm{CHP}}^{\mathrm{g}}(t) \le P_{\mathrm{CHP}}^{\mathrm{g,max}} \end{cases} \tag{23}$$

where $P_{\mathrm{CHP}}^{\mathrm{g}}(t)$ represents the gas supplied to the CHP; $\eta_{\mathrm{CHP}}^{\mathrm{e}}$ and $\eta_{\mathrm{CHP}}^{\mathrm{h}}$ represent the electrical and thermal production efficiency of the CHP; $P_{\mathrm{CHP}}^{\mathrm{e}}(t)$ and $P_{\mathrm{CHP}}^{\mathrm{h}}(t)$ are the electrical and thermal energy produced by the CHP; $P_{\mathrm{CHP}}^{\mathrm{g,max}}$ and $P_{\mathrm{CHP}}^{\mathrm{g,min}}$ denote the maximum and minimum bounds of the gas supplied to the CHP.

(7) Gas boiler

$$\begin{cases} P_{\mathrm{GB}}^{\mathrm{h}}(t) = \eta_{\mathrm{GB}} P_{\mathrm{GB}}^{\mathrm{g}}(t) \\ P_{\mathrm{GB}}^{\mathrm{g,min}} \le P_{\mathrm{GB}}^{\mathrm{g}}(t) \le P_{\mathrm{GB}}^{\mathrm{g,max}} \end{cases} \tag{24}$$

where $P_{\mathrm{GB}}^{\mathrm{g}}(t)$ represents the gas supplied to the GB; η_{GB} denotes the efficiency of heat production in the GB; $P_{\mathrm{GB}}^{\mathrm{h}}(t)$ is the heat energy generated by the GB; $P_{\mathrm{GB}}^{\mathrm{g,max}}$ and $P_{\mathrm{GB}}^{\mathrm{g,min}}$ denote the maximum and minimum bounds of the gas supplied to the GB.

(8) Air conditioner

$$\begin{cases} P_{\mathrm{AC}}^{\mathrm{c}}(t) = \eta_{\mathrm{AC}} P_{\mathrm{AC}}^{\mathrm{e}}(t) \\ P_{\mathrm{AC}}^{\mathrm{e,min}} \le P_{\mathrm{AC}}^{\mathrm{e}}(t) \le P_{\mathrm{AC}}^{\mathrm{e,max}} \end{cases} \tag{25}$$

where $P_{\mathrm{AC}}^{\mathrm{e}}(t)$ represents the electricity supplied to the AC; η_{AC} denotes the efficiency of cooling in the AC; $P_{\mathrm{AC}}^{\mathrm{c}}(t)$ is the cooling power generated by the AC; $P_{\mathrm{AC}}^{\mathrm{e,max}}$ and $P_{\mathrm{AC}}^{\mathrm{e,min}}$ denote the maximum and minimum bounds of the electricity supplied to the AC.

(9) Absorption refrigerator

$$\begin{cases} P_{\mathrm{AR}}^{\mathrm{c}}(t) = \eta_{\mathrm{AR}} P_{\mathrm{AR}}^{\mathrm{h}}(t) \\ P_{\mathrm{AR}}^{\mathrm{h,min}} \le P_{\mathrm{AR}}^{\mathrm{h}}(t) \le P_{\mathrm{AR}}^{\mathrm{h,max}} \end{cases} \tag{26}$$

where $P_{\mathrm{AR}}^{\mathrm{h}}(t)$ represents the heat energy supplied to the AR; η_{AR} denotes the efficiency of cooling in the AR; $P_{\mathrm{AR}}^{\mathrm{c}}(t)$ is the cooling power generated by the AR; $P_{\mathrm{AR}}^{\mathrm{h,max}}$ and $P_{\mathrm{AR}}^{\mathrm{h,min}}$ denote the maximum and minimum bounds of the heat power supplied to the AR.

(10) Multi-source storage

$$\begin{cases} 0 \le P_{ESS}^{\mathrm{j},in}(\mathrm{t}) \le r_{ESS}^{\mathrm{j},in}(\mathrm{t}) \cdot P_{ESS,max}^{\mathrm{j},in} \\ 0 \le P_{ESS}^{\mathrm{j},out}(\mathrm{t}) \le r_{ESS}^{\mathrm{j},out}(\mathrm{t}) \cdot P_{ESS,max}^{\mathrm{j},out} \\ r_{ESS}^{\mathrm{j},in}(\mathrm{t}) + r_{ESS}^{\mathrm{j},out}(\mathrm{t}) = 1 \\ S^{\mathrm{j}}(\mathrm{t}) = S^{j}(\mathrm{t}-1) \cdot (1-\omega^{\mathrm{j}}) + \left(\eta_{ESS}^{j,in} \cdot P_{ESS}^{j,in}(\mathrm{t}) - \frac{P_{ESS}^{j,out}(\mathrm{t})}{\eta_{ESS}^{j,out}} \right) \\ S_{\min}^{j} \le S^{j}(\mathrm{t}) \le S_{max}^{j} \\ S^{j}(1) = S^{j}(\mathrm{T}) \end{cases} \tag{27}$$

where j denotes four distinct categories of energy storage: EES, TES, CES, and GES; $P_{ESS}^{\mathrm{j},in}(\mathrm{t})$ and $P_{ESS}^{\mathrm{j},out}(\mathrm{t})$ represent the storage and release power of the j type of energy storage; $r_{ESS}^{\mathrm{j},in}(\mathrm{t})andr_{ESS}^{\mathrm{j},out}(\mathrm{t})$ are the state variable of the j type of energy storage; $P_{ESS,max}^{\mathrm{j},in}$ and $P_{ESS,max}^{\mathrm{j},out}$ denote the highest storage and release power of the j category of energy storage; $S^{\mathrm{j}}(\mathrm{t})$ is the energy storage capacity of the j category of energy storage; ω^{j} represents the self-discharge rate of the j type of energy storage; $\eta_{ESS}^{j,in}$ and $\eta_{ESS}^{j,out}$ are the storage and release efficiency of the j type of energy storage; S_{max}^{j} and $S_{\min}^{j}$ signify the maximum and minimum capacity of the j type of energy storage.

3.2.2. Power Balance Constraints

(1) Electrical power balance

$$P_{wind}(\mathrm{t}) + P_{\mathrm{pv}}(\mathrm{t}) + P_{Grid}(\mathrm{t}) + P^{\mathrm{e}}_{\mathrm{HFC}}(t) + P^{\mathrm{e}}_{\mathrm{CHP}}(t) + P^{e,out}_{ESS}(\mathrm{t}) = P_{\mathrm{e},L}(\mathrm{t}) + P^{\mathrm{e}}_{\mathrm{EL}}(t) + P^{\mathrm{e}}_{\mathrm{AC}}(t) + P^{e,in}_{ESS}(\mathrm{t}) \quad (28)$$

(2) Thermal power balance

$$P^{\mathrm{h}}_{\mathrm{HFC}}(t) + P^{\mathrm{h}}_{\mathrm{CHP}}(t) + P^{\mathrm{h}}_{\mathrm{GB}}(t) + P^{h,out}_{ESS}(\mathrm{t}) = P_{\mathrm{h},L}(\mathrm{t}) + P^{h,in}_{ESS}(\mathrm{t}) + P^{\mathrm{h}}_{\mathrm{AR}}(t) \quad (29)$$

(3) Gas power balance,

$$P_{\mathrm{Gas}}(\mathrm{t}) + P^{\mathrm{g}}_{\mathrm{MR}}(t) + P^{g,out}_{ESS}(\mathrm{t}) = P_{\mathrm{g},L}(\mathrm{t}) + P^{g,in}_{ESS}(t) + P^{\mathrm{g}}_{\mathrm{CHP}}(t) + P^{\mathrm{g}}_{\mathrm{GB}}(t) \quad (30)$$

(4) Cold power balance

$$P^{\mathrm{c}}_{\mathrm{AC}}(t) + P^{\mathrm{c}}_{\mathrm{AR}}(t) + P^{c,out}_{ESS}(\mathrm{t}) = P_{\mathrm{c},L}(\mathrm{t}) + P^{c,in}_{ESS}(\mathrm{t}) \quad (31)$$

(5) Hydrogen power balance

$$P^{\mathrm{H}}_{\mathrm{EL}}(t) = P^{\mathrm{H}}_{\mathrm{HFC}}(t) + P^{\mathrm{H}}_{\mathrm{MR}}(t) \quad (32)$$

3.3. Model Solution

This paper's optimization scheduling model for the SNLS system belongs to the mixed integer linear programming problems. To address this, the paper opts for the Yalmip toolbox within the MATLAB 2019a platform and utilizes the Cplex 12.10 solver for programming and solving. The model-solving process is depicted in Figure 5.

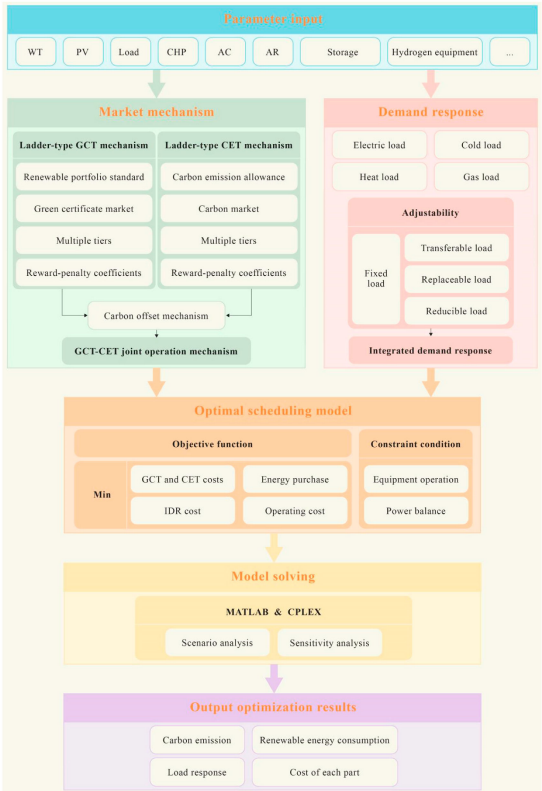

Figure 5. Flowchart of the model-solving process.

4. Case Study

4.1. Basic Data

This paper validates the effectiveness of the proposed optimization scheduling model by conducting a comparative analysis of the SNLS system in diverse scenarios. The forecast values of the system's wind and photovoltaic power output, as well as loads, are detailed in Figure 6. The time-of-use electricity price is provided in Table 1. The parameters of energy conversion units and energy storage units are listed in Tables 2 and 3, respectively, while the parameters of market mechanisms are specified in Table 4.

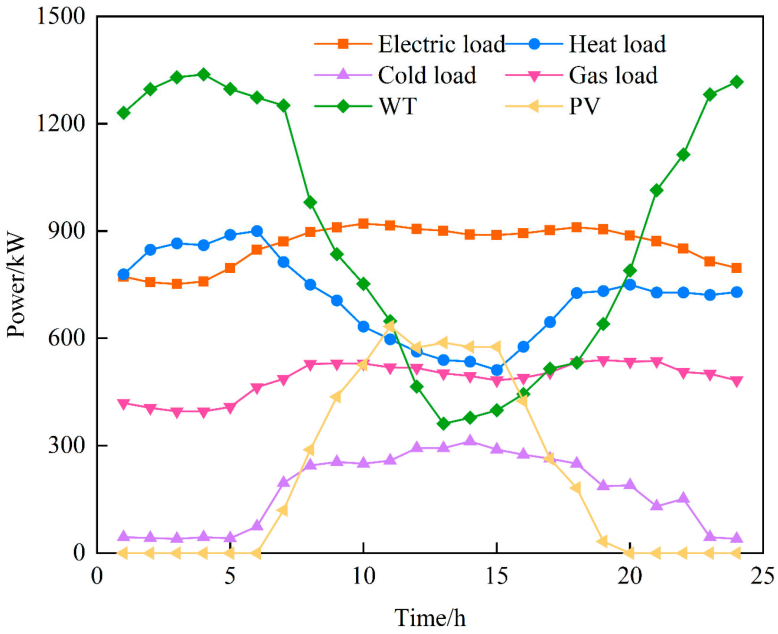

Figure 6. Predicted outputs of wind and photovoltaic energy alongside load forecasts.

Table 1. Time-of-use electricity price.

Type	Time Period	Electricity Price (CNY/kWh)
Valley	01:00–07:00 22:00–24:00	0.48
Flat	07:00–11:00 14:00–18:00	0.88
Peak	11:00–14:00 18:00–22:00	1.10

Table 2. Parameters of energy conversion devices.

Equipment	Capacity(kW)	Energy Conversion Efficiency (%)	Ramp Constraint (%)
EL	500	87	20
HFC	250	Electric: 40 Heat: 55	20
MR	300	65	20
CHP	900	Electric: 40 Heat: 55	20
GB	600	90	20
AC	80	400	20
AR	200	120	20

Table 3. Parameters of energy storage devices.

Equipment	Capacity (kW)	Storage Capacity Upper and Lower Limits (%)	Charging and Discharging Efficiency (%)	Ramp Constraint (%)	Self-Loss Rate (%)
EES	450	90, 10	95	20	1
TES	500	90, 10	95	20	1
GES	300	90, 10	95	20	1
CES	300	90, 10	95	20	1

Table 4. Parameters of the market mechanism.

Parameter	Value	Parameter	Value
Basic price of green certificates (CNY/book)	100	Basic price of carbon trading (CNY/t)	251
Quota coefficient of green certificates	0.20	Price increase range of ladder-type CET	0.25
Price increase range of ladder-type GCT	0.25	Reward coefficient of ladder-type CET	0.20
Reward coefficient of ladder-type GCT	0.20	Interval length of ladder-type CET (t)	2
Interval length of ladder-type GCT (book)	2	Carbon offset upper limit (%)	10
CEA quota coefficient of electricity generation (t/(MWh))	0.728	CEA quota coefficient of heat generation (t/GJ)	0.102
Carbon emission intensity of electricity generation (t/(MWh))	1.08	Carbon emission intensity of heat generation (t/GJ)	0.065

This study establishes six scenarios to compare and analyze the economics, renewable energy penetration, and carbon emission of the SNLS system under each scenario.

Scenario 1: Conventional scheduling model without considering market mechanisms and demand response mechanisms.
Scenario 2: Introducing conventional GCT mechanism on the basis of Scenario 1.
Scenario 3: Introducing ladder-type GCT mechanism on the basis of Scenario 1.
Scenario 4: Introducing ladder-type CET mechanism on the basis of Scenario 3.
Scenario 5: Introducing GCT-CET joint operation mechanism on the basis of Scenario 4.
Scenario 6: Introducing IDR mechanism on the basis of Scenario 5.

The scheduling outcomes for the aforementioned six scenarios are listed in Table 5.

Table 5. Optimization scheduling results for each scenario.

Results	Scenario 1	Scenario 2	Scenario 3	Scenario 4	Scenario 5	Scenario 6
Energy procurement cost (CNY)	11,018	10,376	9898	9921	9913	9340
GCT cost (CNY)	/	−1885	−2552	−2610	−2515	−2604
CET cost (CNY)	/	/	/	−1467	−1754	−1822
System operation cost (CNY)	1255	1955	2707	2927	2953	2765
IDR cost (CNY)	/	/	/	/	/	62
Comprehensive cost (CNY)	12,273	10,446	10,053	8771	8597	7741
Renewable energy penetration (%)	76.46	86.03	95.07	96.90	97.07	100
Carbon emission (kg)	6936	6422	5056	4220	4194	3432

4.2. Analysis of the Effectiveness of the Ladder-Type GCT-CET Joint Operation Mechanism

4.2.1. Effectiveness of the Ladder-Type GCT Mechanism

An analysis of Table 5 and Figure 7 reveals that the introduction and improvement of the GCT mechanism have led to improvements in both the economic and environmental attributes of the SNLS system. In contrast to Scenario 1, the renewable energy penetration increased by 9.57%, the carbon emissions decreased by 514 kg, and the overall system cost decreased by CNY 1827 in Scenario 2. The introduction of the GCT mechanism increases the constraints on green certificate quota indicators and considers the system's GCT revenue, thereby facilitating the penetration of renewable energy and reducing the electricity purchase demand, which subsequently lowers the comprehensive cost. Compared to

Scenario 2, which employs the conventional GCT mechanism, the proposed ladder-type GCT mechanism in Scenario 3 exerts stronger constraints, leading to a further increase of 9.04% in renewable energy penetration and a reduction of 1366 kg in carbon emissions. The proposed ladder-type GCT mechanism utilizes more flexible green certificate trading prices. Consequently, GCT revenue increases with the increase in renewable energy penetration. The system's comprehensive cost decreased by a total of CNY 393 due to the decrease in energy procurement cost. It can be seen from Figure 7 that the implementation of the GCT mechanism promotes the penetration of renewable energy, consequently restricting the purchase of traditional fossil fuels. Improvements in the GCT mechanism enhance the system's capacity to utilize renewable energy, thereby increasing both the economic efficiency of operations and the associated environmental benefits. This validates the effectiveness of the proposed ladder-type GCT mechanism.

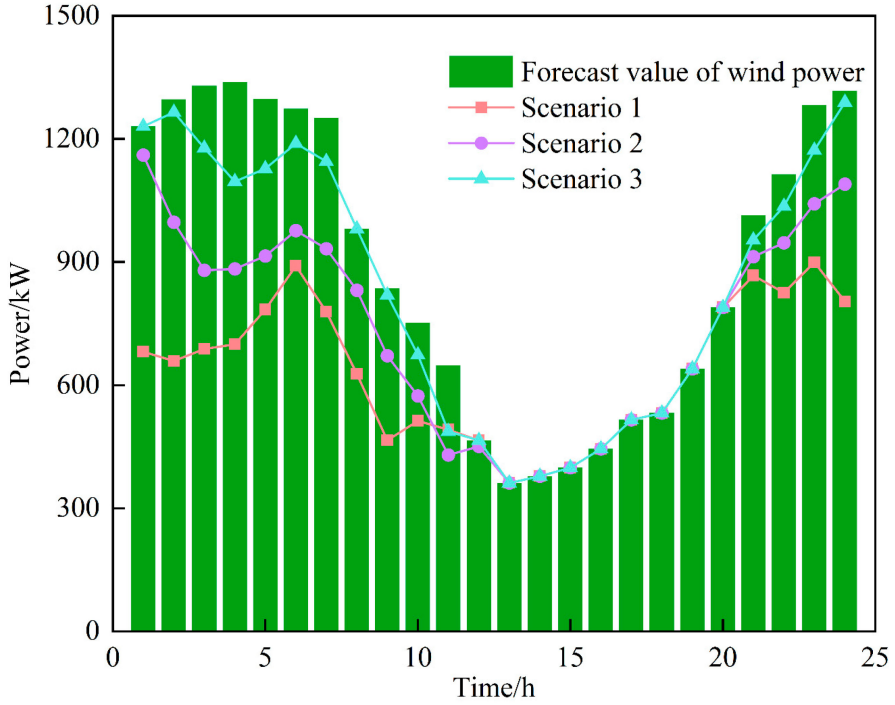

Figure 7. Comparison of renewable energy penetration in Scenarios 1–3.

4.2.2. Effectiveness of the Ladder-Type CET Mechanism

It can be understood from Table 5 that Scenario 4 shows a reduction of 836 kg in carbon emission and a 1.83% increase in renewable energy penetration relative to Scenario 3. The ladder-type CET mechanism increases the scrutiny on the system's carbon emission, strengthening the constraints on carbon emission, thereby reducing the system's willingness to emit carbon and increasing the demand for renewable energy. Furthermore, for units that satisfy the CEA requirements, CET revenue can be generated through the sale of surplus CEA, with the revenue increasing in direct proportion to the quantity of CEA sold. Compared to Scenario 3, which only considers the ladder-type GCT mechanism, Scenario 4 enables the simultaneous gain of GCT and CET revenue, resulting in a reduction of CNY 1282 in the system's comprehensive cost. As depicted in Figure 8, the implementation of the ladder-type CET mechanism further restricts the carbon emission and enhances the system's environmental attributes, thereby validating the effectiveness of the ladder-type CET mechanism proposed in this paper.

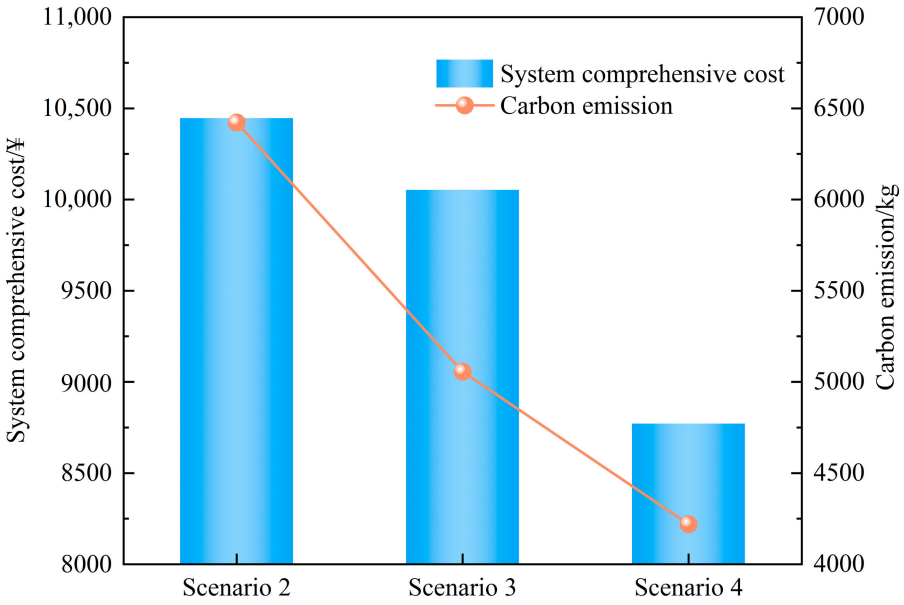

Figure 8. Comparison of system comprehensive cost and carbon emission in Scenarios 2–4.

4.2.3. Effectiveness of the GCT-CET Joint Operation Mechanism

It can be observed from Table 4 and Figure 9 that Scenario 5 shows a decrease of CNY 95 in GCT revenue, accompanied by an increase of CNY 287 in CET revenue, resulting in a net reduction of CNY 174 in the system's comprehensive cost compared to Scenario 4. This is due to the implementation of the GCT-CET joint operation in Scenario 5, which fully considers the environmental benefits associated with green certificates and flexibly allocates redundant green certificates. Under the joint mechanism, surplus green certificates can either participate in the green certificate trading market to generate GCT income or enter the carbon trading market to generate CET income by offsetting carbon emissions. This establishes a channel for green certificates to participate in the CET, breaking down the barriers between the two mechanisms. Furthermore, the environmental benefits associated with green certificates are fully acknowledged, leading to an increased willingness to consume green energy, thereby further reducing the carbon emissions.

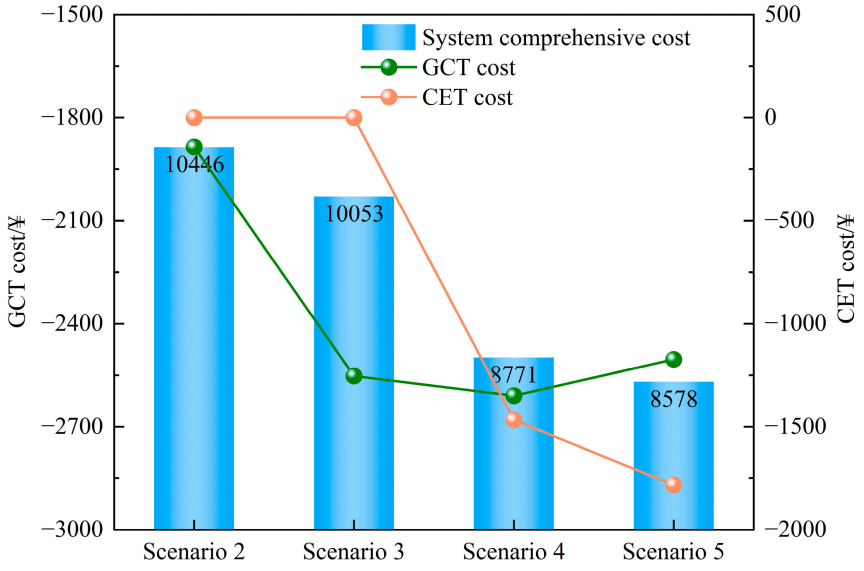

Figure 9. Comparison of GCT cost, CET cost, and system comprehensive cost in Scenarios 2–5.

In summary, the GCT-CET joint operation not only enhances market flexibility, promotes interconnection between different mechanisms, and increases system revenue, but also improves the system's low-carbon attributes, making a significant contribution to the system's green transition. The discussed results validate the effectiveness of the proposed GCT-CET joint operation mechanism in optimizing system economy and low-carbon performance.

4.3. Effectiveness Analysis of IDR Mechanism

From Table 5, it can be seen that the energy purchase cost in Scenario 6 decreased by CNY 573, and the comprehensive cost was reduced by CNY 856 compared to Scenario 5. This is because the IDR mechanism can adjust load levels while satisfying basic energy requirements, thereby alleviating supply–demand imbalances and improving system economics. By analyzing Figures 10 and 11, it can be understood that high wind power generation and low load demand at night allow the IDR mechanism to effectively guide demand-side responses through electricity price information and incentives. Certain thermal and gas loads are substituted by electrical loads, and some daytime electricity and cooling loads are shifted to nighttime, thereby enhancing the utilization of wind power. During the day, when load demand increases, the IDR mechanism reduces electrical loads during high-cost periods, lowering the demand for purchased electricity and thus reducing carbon emissions and system costs. As shown in Figure 11, the implementation of the IDR mechanism effectively improves the system's renewable energy consumption and reduces carbon emission levels, enhances supply–demand matching, and balances the system's economic and environmental performance.

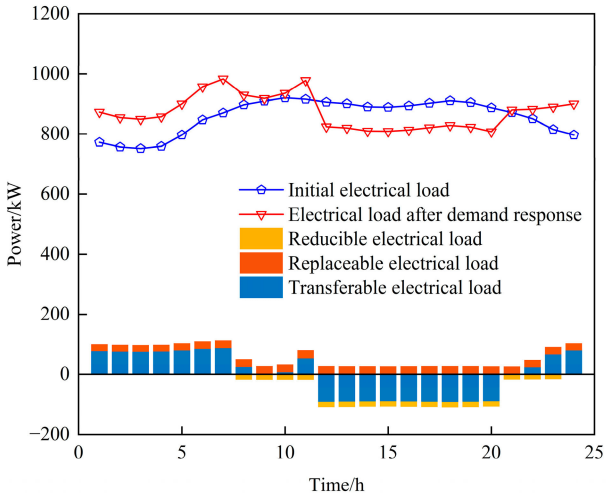

(**a**) Electrical load optimization result

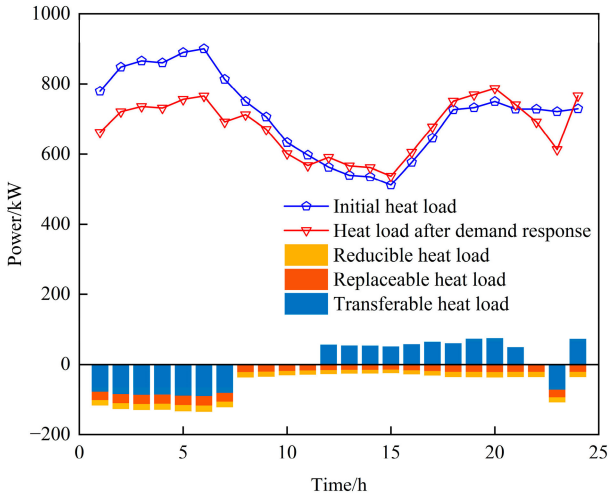

(**b**) Heat load optimization result

Figure 10. *Cont.*

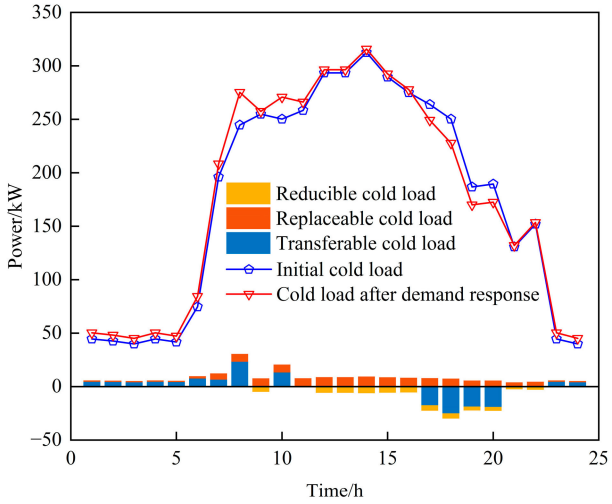

(**c**) Cold load optimization result

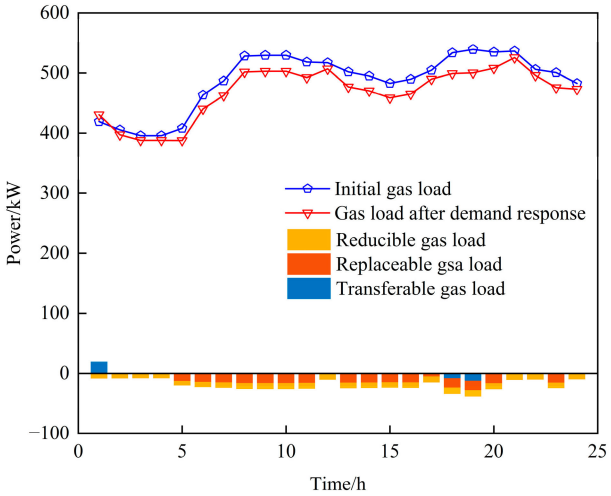

(**d**) Gas load optimization result

Figure 10. Load curve before and after optimization.

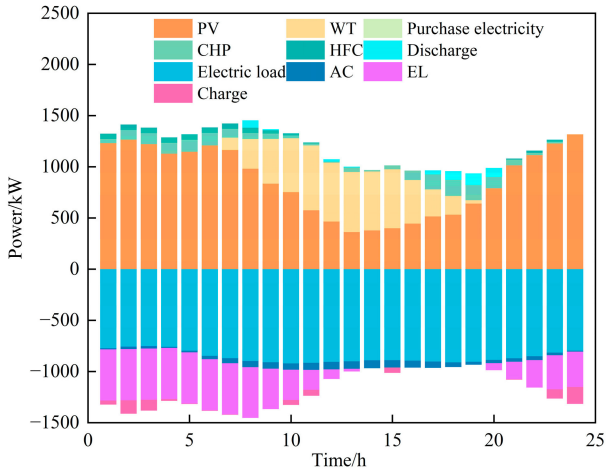

(**a**) Electricity balance result for Scenario 5

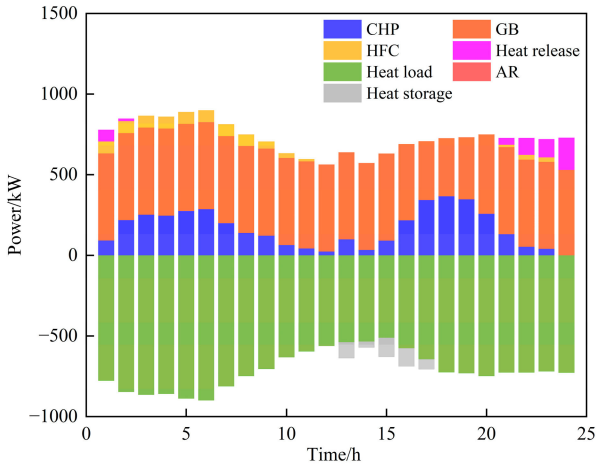

(**b**) Heat balance result for Scenario 5

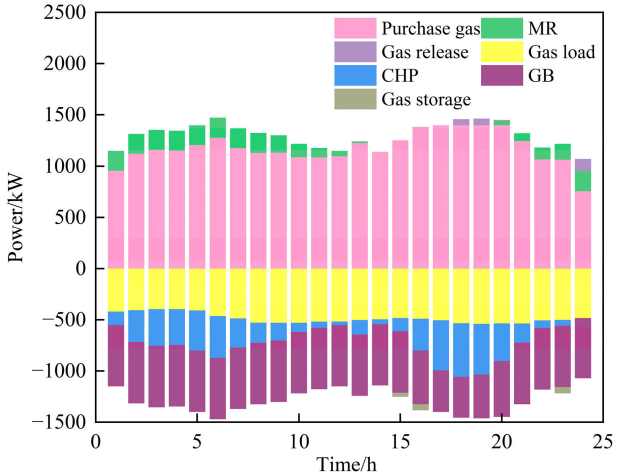

(**c**) Gas balance result for Scenario 5

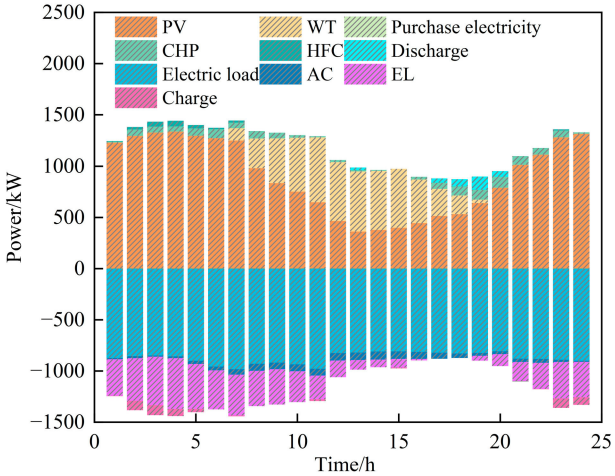

(**d**) Electricity balance result for Scenario 6

Figure 11. *Cont*.

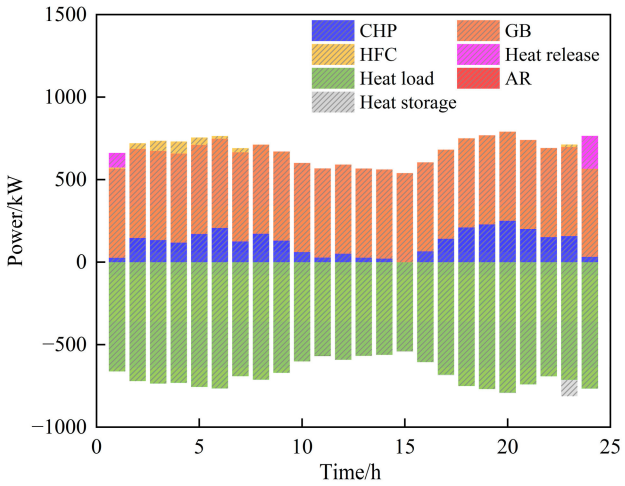

(**e**) Heat balance result for Scenario 6

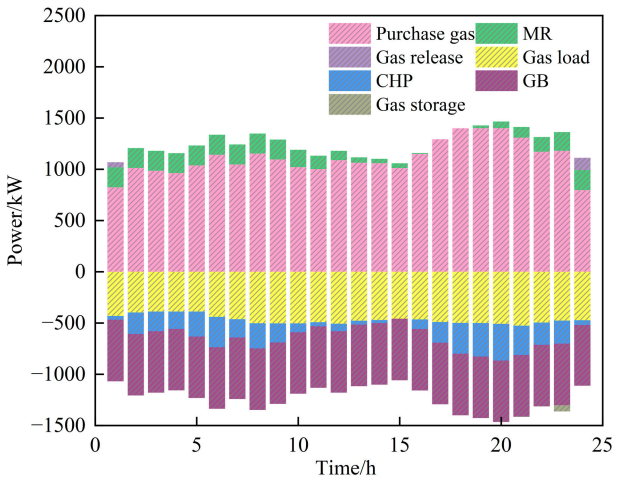

(**f**) Gas balance result for Scenario 6

Figure 11. Optimization result of supply–demand balance.

4.4. Sensitivity Analysis

4.4.1. The Influence of the Green Certificate–Carbon Trading Basic Price on System Operation

The setting of base prices in GCT and CET mechanisms determines their weight in optimization objectives. Effective price setting enhances the system's renewable energy consumption capacity, optimizes carbon emission levels, and ensures economic efficiency. Therefore, it is essential to analyze the scheduling results under different base prices.

Figure 12 shows that when the mechanism prices are relatively low, the system exhibits weak sensitivity to these mechanisms. As prices increase, the influence of both mechanisms grows. To enhance GCT and CET benefits, the system increases its renewable energy consumption capacity and reduces carbon emissions. Additionally, the proposed ladder-type mechanism leads to higher system revenue with improved renewable energy consumption and carbon reduction, resulting in a decrease in comprehensive costs. Once basic prices reach a specific threshold, the system's scheduling capacity becomes limited, and further increases in prices no longer significantly influence the mechanism.

4.4.2. The Influence of Reward Coefficients on System Operation

In the proposed ladder-type mechanism, the appropriate setting of the reward coefficients is crucial for the effectiveness of the mechanisms. Therefore, it is necessary to analyze the scheduling results under different reward coefficients.

Figure 13 illustrates that when the reward coefficients are zero, the system is insensitive to the motivating effects of the two mechanisms. The system's renewable energy consumption is low, while carbon emissions and comprehensive costs are high. With an increase in the reward coefficients, the system's participation in the market grows to achieve higher benefits, thereby enhancing renewable energy consumption, and reducing carbon emissions and comprehensive costs. However, once the reward coefficients reach a certain threshold, the scheduling space becomes constrained, and both renewable energy consumption and carbon emissions tend to stabilize.

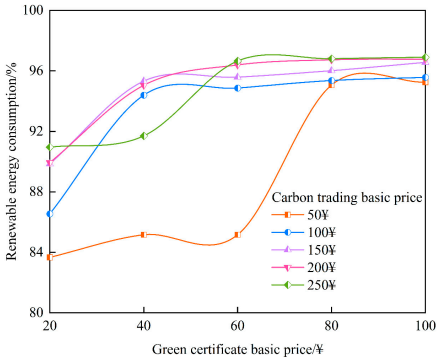

(**a**) Result of renewable energy consumption

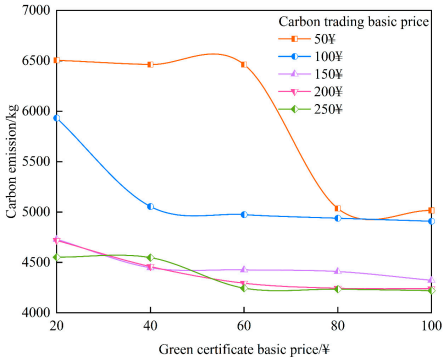

(**b**) Result of carbon emission

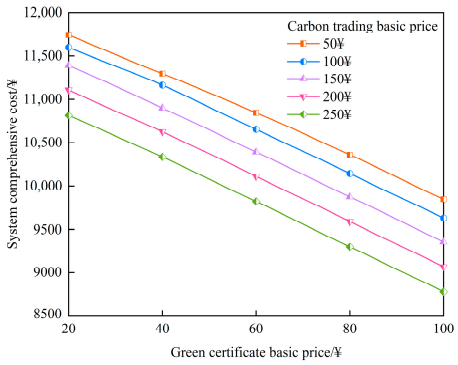

(**c**) Result of system comprehensive cost

Figure 12. Optimization results based on varying green certificate–carbon trading basic prices.

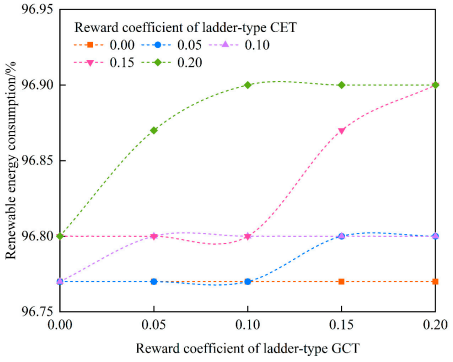

(**a**) Result of renewable energy consumption

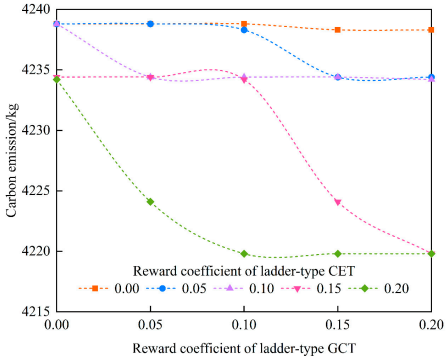

(**b**) Result of carbon emission

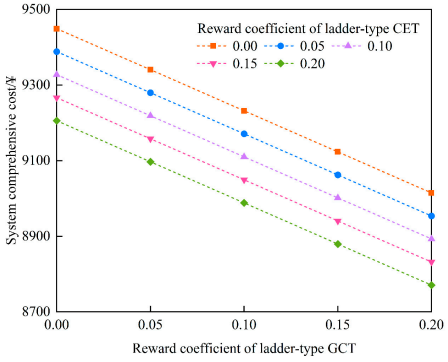

(**c**) Result of system comprehensive cost

Figure 13. Optimization results based on varying reward coefficient.

5. Conclusions

To address the limitation of conventional scheduling strategies, this paper proposes an economic low-carbon optimization scheduling model that considers the ladder-type GCT-CET joint operation and IDR comprehensively. By analyzing the economic and environmental performance of the SNLS system across six scenarios along with sensitivity analysis on key parameters, the following conclusions are drawn:

(1) The proposed ladder-type GCT-CET joint operation mechanism fully leverages the market's role in optimizing scheduling. The ladder-type GCT mechanism offers stronger constraints and greater flexibility, enhancing the system's ability to absorb renewable energy. Additionally, the GCT-CET joint operation mechanism breaks down the barriers between the two market mechanisms, thereby reducing system carbon emissions and costs.

(2) The IDR mechanism employed in this paper fully considers the coupling between multiple sources and the flexibility of flexible loads. The IDR mechanism effectively matches supply and demand through incentives, thereby enhancing renewable energy utilization, reducing carbon emissions, and lowering overall costs.

(3) To ensure the effective implementation of the optimization scheduling strategy in practice, this paper conducts sensitivity analysis on key parameters such as base prices and reward coefficients in market mechanisms. By comparing the impact of different values on the SNLS system's economic and environmental performances, this analysis provides guidance for the rational setting of these parameters.

In summary, this paper leverages the GCT and CET mechanisms to fully utilize market scheduling functions and effectively explores the flexibility of resources on the demand side through the IDR mechanism. This approach provides a viable solution for the green transformation and economic operation of the SNLS systems. Given that the assumptions in this paper may not fully capture the complexities of real-world applications, factors such as market fluctuations, regulatory frameworks, and technological advancements could affect the practical effectiveness of the proposed model. Future research will focus on examining the impacts of source-load uncertainties and market dynamics on scheduling strategies to address these limitations. Such studies would offer deeper insights into the green and sustainable development of energy systems.

Author Contributions: Conceptualization, Z.W. and J.W.; methodology, Z.W. and J.W.; software, Z.W.; validation, Z.W. and Y.K.; formal analysis, Z.W. and H.J.; investigation, Z.W. and M.Z.; resources, Y.K.; data curation, M.Z.; writing—original draft preparation, Z.W.; writing—review and editing, Z.W.; supervision, Y.K. and H.J.; project administration, J.W. All authors have read and agreed to the published version of the manuscript.

Funding: Project supported by the Open project of Key Laboratory in Xinjiang Uygur Autonomous Region of China (2023D04071) and National Natural Science Foundation of China (52167016). Project Supported by Key Research and Development Project of Xinjiang Uygur Autonomous Region (2022B01020-3).

Institutional Review Board Statement: Not applicable.

Informed Consent Statement: Not applicable.

Data Availability Statement: Data are contained within the article.

Acknowledgments: We appreciate the editors and peer reviewers for their constructive comments and will reflect on the shortcomings of this paper.

Conflicts of Interest: Yang Kou and Huan Jiang were employed by Electric Power Research Institute of State Grid Xinjiang Electric Power Co., Ltd. The remaining authors declare that the research was conducted in the absence of any commercial or financial relationships that could be construed as a potential conflict of interest.

Nomenclature

Abbreviations	
SNLS	Source network load storage
GCT	Green certificate trading
CET	Carbon emission trading
IDR	Integrated demand response
P2G	Power to gas
RPS	Renewable portfolio standard
CHP	Combined heat and power
WHB	Waste heat boilers
WT	Wind turbine
PV	Photovoltaic
EL	Electrolyzer
MR	Methane reactor
HFC	Hydrogen fuel cell
GT	Gas turbine
GB	Gas boiler
AC	Air conditioner
AR	Absorption refrigerator
EES	Electrical energy storage
CES	Cold energy storage
TES	Thermal energy storage
GES	Gas energy storage
CEAs	Carbon Emission Allowances
Parameters	
α_P	Quota coefficient of green certificates
α_z	Green certificate conversion coefficient
e	Reward coefficient of ladder-type GCT
u	Price increase range of ladder-type GCT
d	Interval length of ladder-type GCT
σ	CEA quota coefficient
τ_{CHP}	Electro-thermal conversion coefficient of the CHP units
θ	Carbon emission intensity
β	Reward coefficient for ladder-type CET
ε	Price increase range of ladder-type CET
l	Interval length of ladder-type CET
N	Total number of operation and maintenance units
α_n	Unit operating and maintenance cost for different units
η	Energy conversion efficiency
ω^j	Self-discharge rate of the j type of energy storage
S	Energy storage capacity
Variables	
Q_n	Green certificate quota
Q_h	Quantity of green certificates obtained
P	Power
Q_{GCT}	Quantity of green certificates either sold or purchased
λ	Cost
C_{GCT}	Basic price of green certificates
C_{CET}	Carbon trading basic price
E^P	CEA
E_{CET}	Carbon trading volume
Q^*	Surplus green certificate after meeting the green certificate quota
Q_z	Surplus green certificate participating in the carbon offset mechanism
E_{Green}^{CO2}	Amount of carbon emissions offset
E_{CET}^*	Carbon trading volume under the GCT-CET joint operation mechanism
ΔP	Power variation
r	State variable
$C_{Grid}(t)$	Electricity price
$C_{Gas}(t)$	Gas price
Superscripts	
i	Types of load
0	Initial value
L	Load
z	Transferable load
k	Replaceable load
c	Reducible load
max	Maximum value
min	Minimum value
e	Electrical power
H	Hydrogen power
h	Thermal power
g	Gas power
j	Types of energy storage
in	Input power
out	Output power

References

1. Zhao, X.; Ma, X.; Chen, B.; Shang, Y.; Song, M. Challenges toward carbon neutrality in China: Strategies and countermeasures. *Resour. Conserv. Recycl.* **2022**, *176*, 105959. [CrossRef]
2. He, J.; Li, Z.; Zhang, X.; Wang, H.; Dong, W.; Du, E.; Chang, S.; Ou, X.; Guo, S.; Tian, Z.; et al. Towards carbon neutrality: A study on China's long-term low-carbon transition pathways and strategies. *Environ. Sci. Ecotechnology* **2022**, *9*, 100134. [CrossRef] [PubMed]
3. Fan, H.; Yu, Z.; Xia, S.; Li, X. Review on coordinated planning of source-network-load-storage for integrated energy systems. *Front. Energy Res.* **2021**, *9*, 641158. [CrossRef]
4. Feng, T.T.; Li, R.; Zhang, H.M.; Gong, X.L.; Yang, Y.S. Induction mechanism and optimization of tradable green certificates and carbon emission trading acting on electricity market in China. *Resour. Conserv. Recycl.* **2021**, *169*, 105487. [CrossRef]
5. Golmohamadi, H. Demand-side flexibility in power systems: A survey of residential, industrial, commercial, and agricultural sectors. *Sustainability* **2022**, *14*, 7916. [CrossRef]

6. Yang, M.; Liu, Y. Research on multi-energy collaborative operation optimization of integrated energy system considering carbon trading and demand response. *Energy* **2023**, *283*, 129117. [CrossRef]
7. Dziejarski, B.; Krzyżyńska, R.; Andersson, K. Current status of carbon capture, utilization, and storage technologies in the global economy: A survey of technical assessment. *Fuel* **2023**, *342*, 127776. [CrossRef]
8. Ikäheimo, J.; Weiss, R.; Kiviluoma, J.; Pursiheimo, E.; Lindroos, T.J. Impact of power-to-gas on the cost and design of the future low-carbon urban energy system. *Appl. Energy* **2022**, *305*, 117713. [CrossRef]
9. Farhat, O.; Faraj, J.; Hachem, F.; Castelain, C.; Khaled, M. A recent review on waste heat recovery methodologies and applications: Comprehensive review, critical analysis and potential recommendations. *Clean. Eng. Technol.* **2022**, *6*, 100387. [CrossRef]
10. Yang, D.; Xu, Y.; Liu, X.; Jiang, C.; Nie, F.; Ran, Z. Economic-emission dispatch problem in integrated electricity and heat system considering multi-energy demand response and carbon capture technologies. *Energy* **2022**, *253*, 124153. [CrossRef]
11. Chen, M.; Lu, H.; Chang, X.; Liao, H. An optimization on an integrated energy system of combined heat and power, carbon capture system and power to gas by considering flexible load. *Energy* **2023**, *273*, 127203. [CrossRef]
12. Liu, Z.; Li, C. Low-carbon economic optimization of integrated energy system considering refined utilization of hydrogen energy and generalized energy storage. *Energies* **2023**, *16*, 5700. [CrossRef]
13. Chen, H.; Yang, S.; Chen, J.; Wang, X.; Li, Y.; Shui, S.; Yu, H. Low-carbon environment-friendly economic optimal scheduling of multi-energy microgrid with integrated demand response considering waste heat utilization. *J. Clean. Prod.* **2024**, *450*, 141415. [CrossRef]
14. Yu, X.; Ge, S.; Zhou, D.; Wang, Q.; Chang, C.T.; Sang, X. Whether feed-in tariff can be effectively replaced or not? An integrated analysis of renewable portfolio standards and green certificate trading. *Energy* **2022**, *245*, 123241. [CrossRef]
15. Li, J.; Mao, T.; Huang, G.; Zhao, W.; Wang, T. Research on day-ahead optimal scheduling considering carbon emission allowance and carbon trading. *Sustainability* **2023**, *15*, 6108. [CrossRef]
16. Zhu, X.; Xue, J.; Hu, M.; Liu, Z.; Gao, X.; Huang, W. Low-carbon economy dispatching of integrated energy system with P2G-HGT coupling wind power absorption based on stepped carbon emission trading. *Energy Rep.* **2023**, *10*, 1753–1764. [CrossRef]
17. Gao, J.; Meng, Q.; Liu, J.; Wang, Z. Thermoelectric optimization of integrated energy system considering wind-photovoltaic uncertainty, two-stage power-to-gas and ladder-type carbon trading. *Renew. Energy* **2024**, *221*, 119806. [CrossRef]
18. Zhang, L.; Liu, D.; Cai, G.; Lyu, L.; Koh, L.H.; Wang, T. An optimal dispatch model for virtual power plant that incorporates carbon trading and green certificate trading. *Int. J. Electr. Power Energy Syst.* **2023**, *144*, 108558. [CrossRef]
19. Yasmin, R.; Amin, B.M.R.; Shah, R.; Barton, A. A survey of commercial and industrial demand response flexibility with energy storage systems and renewable energy. *Sustainability* **2024**, *16*, 731. [CrossRef]
20. Chen, Z.; Chen, Y.; He, R.; Liu, J.; Gao, M.; Zhang, L. Multi-objective residential load scheduling approach for demand response in smart grid. *Sustain. Cities Soc.* **2022**, *76*, 103530. [CrossRef]
21. Bin, L.; Shahzad, M.; Javed, H.; Muqeet, H.A.; Akhter, M.N.; Liaqat, R.; Hussain, M.M. Scheduling and sizing of campus microgrid considering demand response and economic analysis. *Sensors* **2022**, *22*, 6150. [CrossRef]
22. Guo, W.; Xu, X. Comprehensive energy demand response optimization dispatch method based on carbon trading. *Energies* **2022**, *15*, 3128. [CrossRef]